



Journal of Catalysis Vol. 266, Issue 1, 2009

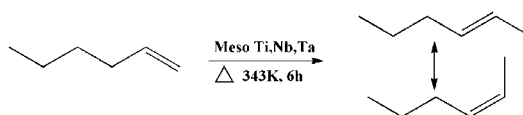
Contents

REGULAR ARTICLES

Investigation of the catalytic activities of sulfated mesoporous Ti, Nb, and Ta oxides in 1-hexene isomerization

pp 1–8

Yuxiang Rao, Junjie Kang, Michel Trudeau, David M. Antonelli*

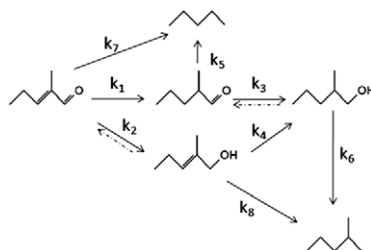


Amine templated mesoporous transition metal oxides (Ti, Nb, and Ta) with different pore sizes were synthesized and evaluated in 1-hexene isomerization reaction for their catalytic activities and selectivities toward 2-hexene isomers.

Hydrogenation and Hydrodeoxygenation of 2-methyl-2-pentenal on supported metal catalysts

pp 9–14

Trung T. Pham, Lance L. Lobban, Daniel E. Resasco, Richard G. Mallinson*

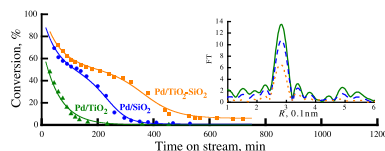


Hydrodeoxygenation and hydrogenolysis of 2-methyl-2-pentenal have been studied on supported Pt, Pd, and Cu catalysts. The activity followed the order Pt > Pd > Cu. Major products were 2-methyl-pentanal, 2-methyl-2-pentenol and 2-methyl-pentanol. *n*-Pentane was produced on Pt and Pd while 2-methyl-pentane is produced on Cu. At very low conversion, Cu showed strong initial hydrogenation activity of C=O to form 2-methyl-2-pentenol.

Sulfur resistance enhancement by grafted TiO₂ in SiO₂-supported Pd catalysts: Role of grafted TiO₂ and genesis of Pd clusters

pp 15–25

Hwo-Shuenn Sheu, Jyh-Fu Lee, Shin-Guang Shyu, Wha-Wen Chou, Jen-Ray Chang*

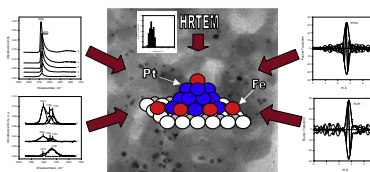


Layer-like TiO₂ clusters increase the roughness of SiO₂, thereby maintaining Pd in high dispersion and increasing catalyst stability during sulfur poisoning.

The effect of Fe on SiO₂-supported Pt catalysts: Structure, chemisorptive, and catalytic properties

pp 26–38

Attilio Siani, Oleg S. Alexeev*, Gwendoline Lafaye, Michael D. Amiridis*

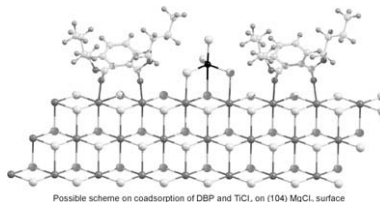


A family of PtFe/SiO₂ samples with different Pt/Fe ratios was prepared and characterized by hydrogen chemisorption, EXAFS, FTIR and catalytic activity measurements for the oxidation of CO, the dehydrogenation of cyclohexane, and the selective hydrogenation of citral. The fraction of Pt–Fe bimetallic contributions in these samples, the nature and extent of electronic interactions between Pt and Fe, and the strength of the CO adsorption on Pt depend strongly on the Fe content, and in turn, affect significantly the catalytic performance of Pt.

Supported Ziegler–Natta catalysts for propylene polymerization. Study of surface species formed at interaction of electron donors and TiCl₄ with activated MgCl₂

pp 39–49

Denis V. Stukalov*, Vladimir A. Zakharov, Alexander G. Potapov, Gennady D. Bukatov

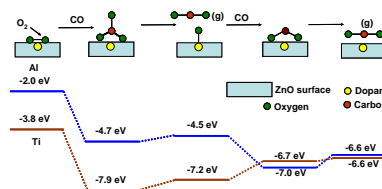


Coadsorption of dibutyl phthalate (DBP) and TiCl₄ on the MgCl₂ (1 0 4) surface.

CO oxidation by Ti- and Al-doped ZnO: Oxygen activation by adsorption on the dopant

pp 50–58

Raj Ganesh S. Pala, Wei Tang, Michael M. Sushchikh, Jung-Nam Park, Arnold J. Forman, Guang Wu, Alan Kleiman-Shwarsstein, Jingping Zhang, Eric W. McFarland, Horia Metiu*

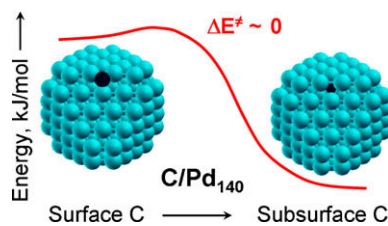


ZnO doped with Ti oxidizes CO by a new mechanism: O₂ adsorbs on the dopant and is activated. This is likely to work when high-valence dopants replace low-valence cations.

Edge sites as a gate for subsurface carbon in palladium nanoparticles

pp 59–63

Francesc Viñes, Christoph Loschen, Francesc Illas, Konstantin M. Neyman*

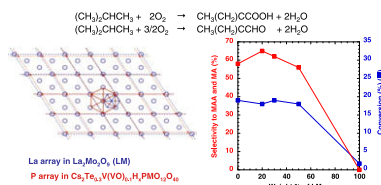


Activation barriers for subsurface migration of C atoms that almost vanish at edges of Pd nanoparticles control the initial stage of carbon incorporation in the catalysts. The potential energy curve for diffusion of *surface* atom C from a near-edge *fcc* site on (1 1 1) facet of Pd₁₄₀ particle via a very low barrier to more stable *subsurface* octahedral interstitial site is shown.

Atypical synergetic effect between Te- and V-substituted phosphomolybdic cesium salt and LAMOX-type phases for the oxidation of isobutane into methacrylic acid

pp 64–70

Q. Huynh, A. Selmi, G. Corbel, P. Lacorre, J.M.M. Millet *

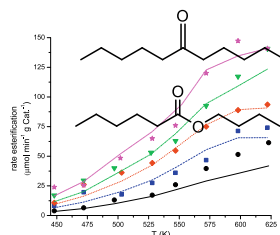


A synergetic effect was found between a phosphomolybdic cesium salt containing VO and Te counteranions and a lanthanum molybdate in isobutane oxidation. It was attributed to crystallographic fits between phases.

Catalytic coupling of carboxylic acids by ketonization as a processing step in biomass conversion

pp 71–78

Christian A. Gaertner, Juan Carlos Serrano-Ruiz, Drew J. Braden, James A. Dumesic *

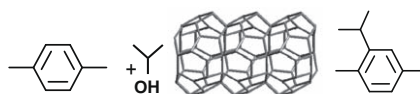


Ketonization and esterification of biomass-derived carboxylic acids have been studied over a ceria–zirconia catalyst, and the coupling between these reactions has been described by a simple kinetic model.

The role of the zeolite channel architecture and acidity on the activity and selectivity in aromatic transformations: The effect of zeolite cages in SSZ-35 zeolite

pp 79–91

Naděžda Žilková, Martina Bejbllová, Barbara Gil, Stacey I. Zones, Allen W. Burton, Cong-Yan Chen, Zuzana Musilová-Pavlačzková, Gabriela Košová, Jiří Čejka *

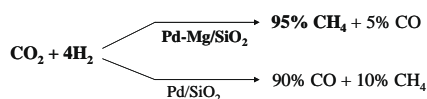


The particular catalytic behavior of SSZ-35 (STF) in toluene and *p*-xylene alkylation and toluene disproportionation is reported. The presence of 18-ring cages ensures high activities/selectivities and substantial resistance against deactivation.

A highly dispersed Pd–Mg/SiO₂ catalyst active for methanation of CO₂

pp 92–97

Jung-Nam Park, Eric W. McFarland *

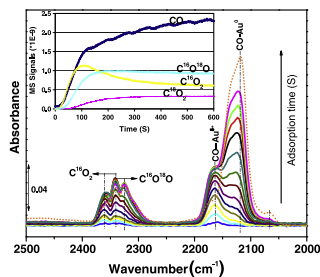


In methanation of carbon dioxide with hydrogen, at 450 °C the Pd-Mg/SiO₂ catalyst has 95% selectivity to CH₄ at a CO₂ conversion of 59%, whereas Pd supported on silica reduces CO₂ primarily to CO, and Mg/SiO₂ alone is inactive.

CO oxidation on Au/FePO₄ catalyst: Reaction pathways and nature of Au sites

pp 98–105

Meijun Li, Zili Wu, Zhen Ma, Viviane Schwartz, David R. Mullins, Sheng Dai, Steven H. Overbury *

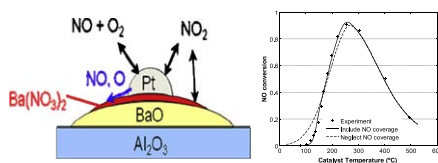


The unusual surface redox property of Au/FePO₄ provides a new pathway for CO oxidation at room temperature, i.e., CO reaction with structural oxygen of FePO₄ via Mars–van Krevelen mechanism in addition to the conventional direct reaction with fed O₂.

Experimental and kinetic study of NO oxidation on model Pt catalysts

pp 106–119

Divesh Bhatia, Robert W. McCabe, Michael P. Harold *, Vemuri Balakotaiah *

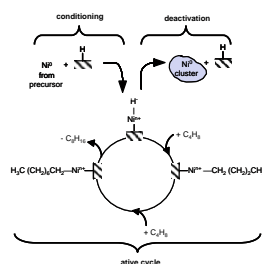


NO oxidation on Pt/Al₂O₃ and Pt/BaO/Al₂O₃ is inhibited by NO and NO₂, and limited by kinetic (O₂ adsorption) and thermodynamic factors. The transient kinetics are further complicated by uptake of NO₂ on both Al₂O₃ and BaO and oxidation of Pt. A global kinetic model is developed to predict the pseudo steady-state NO oxidation rate.

The role of different Ni sites in supported nickel catalysts for butene dimerization under industry-like conditions

pp 120–128

A. Brückner *, U. Bentrup, H. Zanthoff, D. Maschmeyer

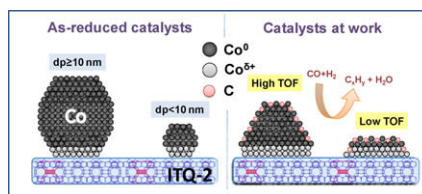


Active sites for butene dimerization are single Niⁿ⁺ (n = 1 and/or 2) moieties which are formed by oxidative addition of Brønsted sites to Ni⁰ precursor species during conditioning and destroyed by reaggregation to Ni⁰ clusters during deactivation. Octene is formed by subsequent insertion of butene into the Ni–H bond followed by β–H elimination.

Cobalt particle size effects in Fischer–Tropsch synthesis: structural and *in situ* spectroscopic characterisation on reverse micelle-synthesised Co/ITQ-2 model catalysts

pp 129–144

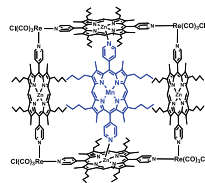
Gonzalo Prieto, Agustín Martínez *, Patricia Concepción, Ramón Moreno-Tost



CO-FTIR studies *in situ* and on working Co/ITQ-2 model catalysts suggest a C-driven surface cobalt reconstruction under Fischer–Tropsch synthesis, irrespective of Co particle size. Interfacial metal-support Co²⁺ sites are favoured due to nanoparticle flattening, and are proposed as responsible for the decreased TOF for particles of size < 10 nm.

Microkinetic analysis of the epoxidation of styrene catalyzed by (porphyrin)Mn encapsulated in molecular squares pp 145–155

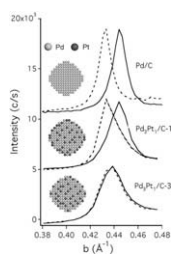
Gloria A.E. Oxford, María C. Curet-Arana, Debarshi Majumder, Richard W. Gurney, Melissa L. Merlau, SonBinh T. Nguyen, Randall Q. Snurr, Linda J. Broadbelt*



Microkinetic modeling showed that deactivation of (porphyrin)Mn catalysts adds significant complexity to the reaction kinetics. (Porphyrin)Mn catalysts encapsulated in molecular squares prevented deactivation of the catalyst, and were found to be the primary catalytic species in this system.

Surface and structure characteristics of carbon-supported Pd₃Pt₁ bimetallic nanoparticles for methanol-tolerant oxygen reduction reaction pp 156–163

Wenming Wang, Qinghong Huang, Juanying Liu, Zhiqing Zou, Miaoying Zhao, Walter Vogel, Hui Yang*



The surface and structure of Pd/Pt nanoparticles can be tuned to optimize the oxygen reduction activity and the tolerance towards methanol in fuel cell applications.

CORRIGENDUM**Corrigendum to “Hydrochlorination of acetylene using supported bimetallic Au-based catalysts” [J. Catal. 257 (2008) 190–198]** p 164

Marco Conte, Albert F. Carley, Gary Attard, Andrew A. Herzing, Christopher J. Kiely, Graham J. Hutchings*